Measurement of the structure of potential cluster bands and absolute branching ratios of high-energy states in ^{18}O*

S. Pirrie[1]**, C. Wheldon**[1]**, Tz. Kokalova**[1]**, J. Bishop**[1]**,
R. Hertenberger**[2]**, H.-F. Wirth**[2]**, S. Bailey**[1]**, N. Curtis**[1]**,
D. Dell'Aquila**[3]**, Th. Faestermann**[4]**, D. Mengoni**[5]**, R. Smith**[1]**,
D. Torresi**[1]**, A. Turner**[1]

[1] School of Physics and Astronomy, University of Birmingham, Edgbaston Park Rd,
Birmingham, UK, B15 2TT
[2] Fakultät für Physik, Ludwig-Maximilians-Universität München, D-85748 Garching, Germany
[3] Università degli Studi di Napoli Federico II, Corso Umberto I, 40, 80138 Napoli NA, Italy
[4] Physik Department, Technische Universität München, D-85748 Garching, Germany
[5] Università degli Studi di Padova, Via 8 Febbraio 1848, 2, 35122 Padova PD, Italy

E-mail: `S.Pirrie@PGR.bham.ac.uk`

Abstract. The investigation of nuclei with potential α-cluster structure is of great importance to the understanding of nuclear structure, both in the testing of theoretical models and for the study of the synthesis of elements in stars. The ^{18}O nucleus is an excellent candidate to test for such a system, and an experiment has been performed in order to determine the validity of proposed cluster bands in ^{18}O, by measuring absolute branching ratios for high-energy excited states. In order to accurately measure these branching ratios, Monte-Carlo techniques have been employed allowing for the precision reproduction of data gathered throughout the experiment. An in-depth description of the considerations required when simulated data for these experiments and comparisons between features in real and simulated data are presented.

1. Introduction

The measurement and determination of exotic nuclear configurations is of vital importance and great interest in the nuclear physics community, elucidating information on the interactions of nucleons within the nuclear system. In particular, systems with cluster configurations present exciting physics outside of the nuclear shell-model, in addition to providing helpful tests of theoretical models due to the reduction in the necessary degrees of freedom. The nucleus ^{18}O is, theoretically, an excellent cluster candidate, in part due to the properties of the ^{14}C nucleus. The ^{16}O nucleus is a commonly proposed cluster, as like the α particle it is doubly magic and has a first excited state at a high excitation energy ($>$6 MeV for ^{16}O), and it has been successfully used in theoretical calculations to reproduce levels; for example, the ^{16}O $\otimes$ α system in ^{20}Ne [1–3]. Similarly, ^{14}C presents p-shell closure and a first excited state at $>$6 MeV, providing strong evidence for its potential as a cluster [4].

An experiment performed by von Oertzen *et al* at the Maier Leibnitz Laboratory (MLL) in Munich, through use of the Q3D (named for the constituent magnets: quadrupole,

dipole, dipole, dipole) magnetic spectrograph, discovered $\approx$30 new states in ^{18}O through use of the ^{12}C(^{7}Li,p)^{18}O* reaction [4]. Rotational bands were then proposed through use of rotational fitting using both new and previously measured states, some with proposed α-cluster configurations: the $K^\pi = 0_2^{+/-}$ with proposed structure ^{14}C $\otimes$ α [5,6] and the $K^\pi = 0_4^{+/-}$ with proposed structure ^{12}C $\otimes$ $2n$ $\otimes$ α [7,8].

In order to determine the validity of the assignments for these states, an experiment to measure the branching ratios of the high-energy states in ^{18}O was performed to ascertain the tendency of these states towards α-clustering. By comparing the measured reduced partial α-decay widths to the Wigner limit, the likelihood of a preformed α particle existing in the appropriate nuclear configuration could be determined [9].

2. Experimental method

To measure the associated branching ratios, the Q3D magnetic spectrograph at MLL was used in conjunction with an array of high-resolution double-sided silicon strip detectors (DSSDs). The positioning of these relative to the beam axis is shown in Figure 1. The ^{12}C(^{7}Li,p)^{18}O* reaction was utilised, through use of a 44.0 MeV ^{7}Li beam produced by the tandem Van de Graaff accelerator at MLL incident on a ^{12}C target under vacuum. This reaction was separated from other reaction channels through particle identification provided by the focal plane detector at the end of the Q3D, described in more detail in reference [11]. Once a proton had been confirmed to be incident at the focal plane detector, the measured position could be calibrated to give the excitation spectra for various energy ranges in ^{18}O. Five regions were investigated:
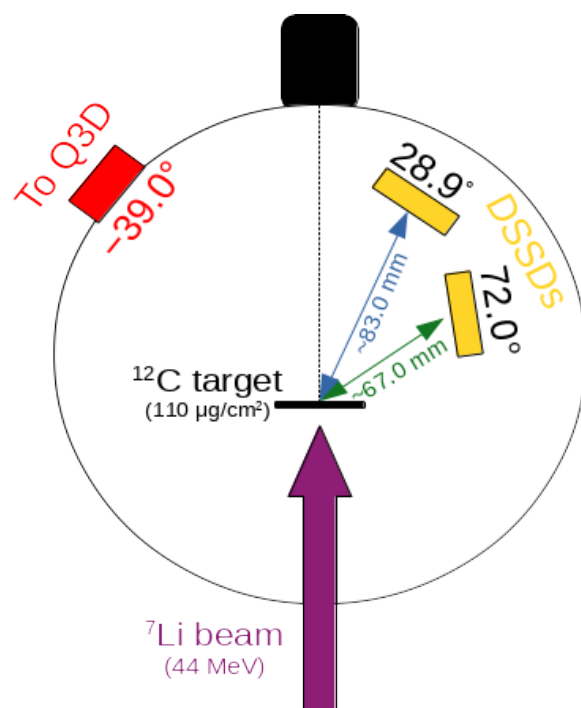

Figure 1. A plan view of the experimental set-up used, with in-plane angles shown. The Q3D magnetic spectrograph was set at $-39°$ in-plane, with an acceptance of $\pm3°$, and at $0°$ out-of-plane, with an acceptance of $\pm2°$. Image adapted from [10].
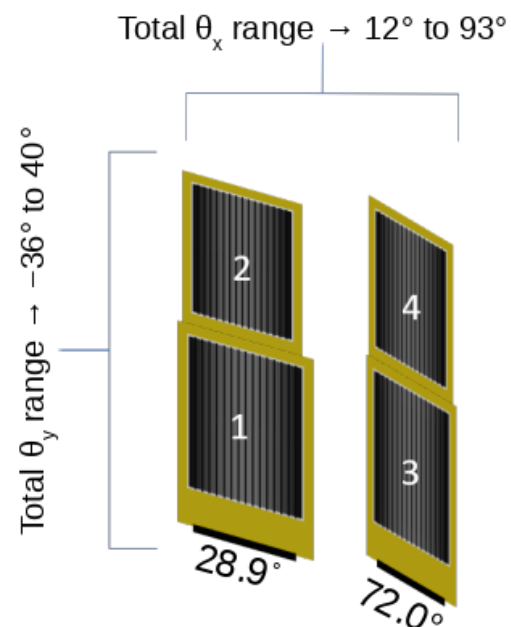
Figure 2. A depiction of the DSSD array, showing how the 4 detectors were placed and the total angular range of the array. Image adapted from [10].

these were centred at 0.8 MeV, 7.8 MeV, 10.5 MeV, 13.2 MeV and 15.1 MeV respectively, thus enabling many states to be measured. The break-up fragments from the ^{18}O corresponding to a proton detection at the Q3D focal plane would then typically be detected by the DSSD array. The angular acceptance and positioning of this array is shown in Figure 2.

3. Monte-Carlo simulations

In order to determine the absolute branching ratios for states in ^{18}O, it was critical that the geometric efficiency of the DSSD array was determined accurately. This was done through Monte-Carlo simulation, using an unpublished in-house package called Resolution8.1 [12–15]. This package simulates thin target nuclear reactions, including direct and compound reactions, at non-relativistic energies. Different angular distributions for the fragments, such as a uniform distribution for compound reactions, can be selected in order to best reproduce data.

The reaction mechanism for break-up reactions follows a multi-step sequential 2-body decay method, allowing for complicated decay chains to be simulated in their entirety. Using the user-inputted masses and charges of the reaction entrance and exit channels, along with the associated Q-value, energies are calculated for the reaction product nuclei and travel along a direction sampled randomly depending on the chosen form of angular distribution. This continues until all nuclei remaining are final-state nuclei. Reaction products can also be left in a user-defined excited state, with an excitation energy smeared by a user-defined width corresponding to Gaussian distribution. Final-state particles can have information outputted in two ways: either with a kinetic energy, θ_x and θ_y or in terms of the momenta along each of the Cartesian axes.

Resolution8.1 also allows for many real-world smearing effects to be considered, producing a more realistic data set for comparison with experimental resolution effects. The available smearing effects are:

- Beam energy spread from the accelerator
- Divergence of the beam from the entrance of the chamber
- Energy loss of the beam and fragments in the target
- Energy straggle of the beam and fragments in the target
- Angular straggle of the beam and fragments in the target
- Recoil due to in-flight γ-decay
- The size and shape of the beam spot.

3.1. Experimental comparisons

Resolution8.1 runs for a user-specified amount of good events, an event in which a proton enters the Q3D based on its angular acceptance (a range of $-42°$ to $-36°$ in x and $-2°$ to $+2°$ in y), while generating no bad events in order to speed up the process of producing the data. For accurate reproduction of the data, it was necessary to assume any protons enter the Q3D at the centre of the acceptance, as this is the largest cause of experimental uncertainty.

In order to give the best agreement between Monte-Carlo and real data, detectors were simulated through use of the same detector processing code used for the real data. Events were read out in terms of kinetic energy and Cartesian angles, which were considered detected if they were travelling in the direction of a detector in the array. Events in which all fragments were outside of the acceptance of the DSSD array were counted to enable estimation of the geometric efficiency. Fragments incident within the acceptance of the array were assigned a vertical and horizontal strip on a DSSD, based on their angle. Once a fragment had been assigned a strip, the position of the fragment was smeared across the 3 mm width of that strip, in order to recreate the angular resolution available in the experiment. The energy of the
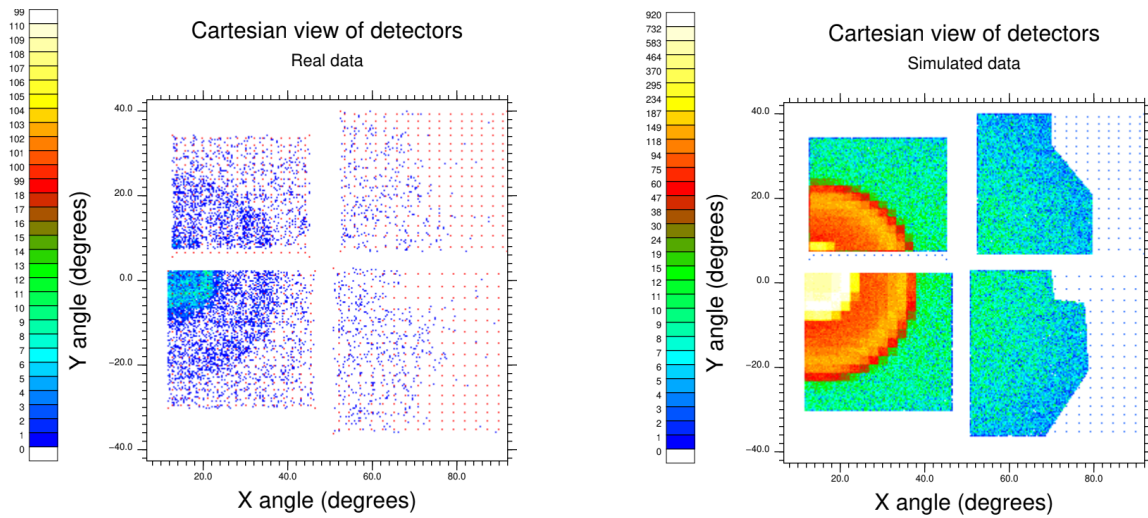
Figure 3. A comparison of the 2D Cartesian views of the detector array, showing the intensity of particles incident on each segment of the detectors, for states in the 10.5 MeV excitation region with real (left) and simulated (right) data. The centres of pseudopixels are also shown. The right hand side of the detector array was blocked by the target ladder in the vacuum chamber in the real data, a feature that is recreated in the simulated data.

simulated fragment was then smeared using a Gaussian distribution, defined by the measured energy resolution of the detector when beam was incident on the target. Other detector effects, such as low-energy thresholds or missing strips on the face of the detectors, were also reproduced. All of these considerations allowed for accurate determination of the angle and position of the DSSDs in the array, by comparing Gaussian profiles of detected decay fragments pixel-by-pixel. A comparison of experimental and simulated data incident on the DSSD array is presented in Figure 3, demonstrating the excellent agreement generated through use of the Monte-Carlo techniques.

In order to identify species detected by the DSSD array, a kinematic methodology known as a Catania plot was employed. This methodology is described in references [10, 16], and involves using conservation of energy and momentum to reconstruct an undetected particle. For the total reaction $^{12}\mathrm{C}(^{7}\mathrm{Li},p)A + B$, where the $^{18}\mathrm{O}^*$ has decayed into particles A and B, the Q-value is given by:

$$Q = E_p + E_A + E_B - E_{beam}, \tag{1}$$

where E is the energy of an associated particle. In this case of a two-body decay into A and B, if A is measured in the DSSD array then due to the energy and position information gathered it is possible to reconstruct the energy and momentum of B by assuming the mass of A, m_A. By plotting the energy $E_p + E_A - E_{beam}$ against half the square of the reconstructed total momentum of B, p_B^2, a locus described by a gradient of $\frac{1}{m_B}$ and an intercept of $-Q$ is produced. If the assumption about m_A is incorrect, events will form a locus not described by this line. An example of this method is shown in Figure 4, where A and B are $^{14}\mathrm{C}$ and α respectively, thus the gradient of the correct locus is given by $\frac{1}{m_B}$ and the intercept by $-Q$ for the total reaction, -2.173 MeV.

Also shown in Figure 4 is a comparison of real data to Monte-Carlo simulation, both in the case with all smearing effects turned off (including effects due to both angle and energy resolution
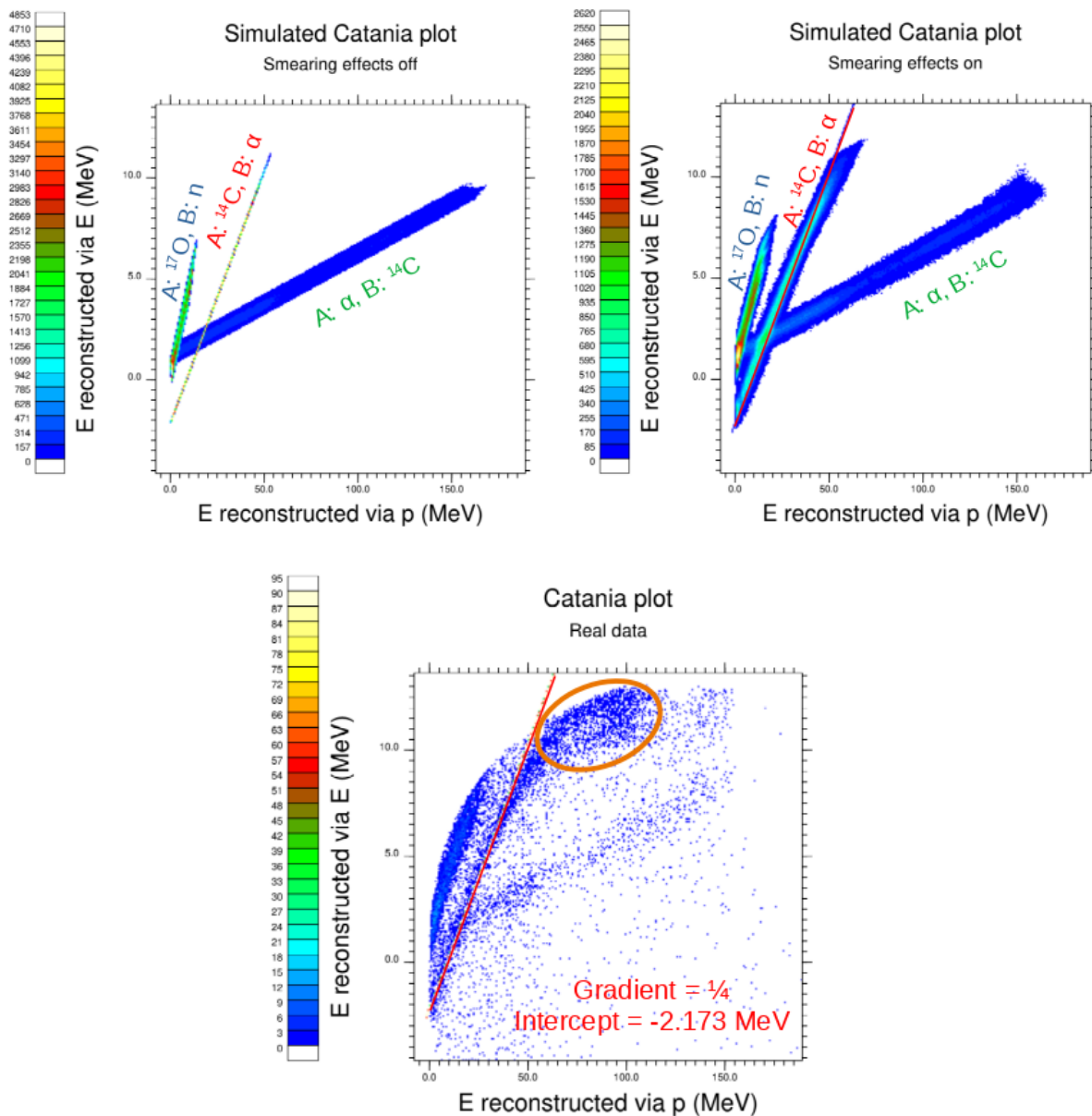
Figure 4. A comparison of the Catania plot produced using real data (bottom) with the simulated Catania plots produced without smearing effects (left) and with smearing effects (right) for all states in the 10.5 MeV excitation region, assuming a detected ^{14}C and reconstructed α. The red line on the real data and smearing-on plots represents a line with gradient $\frac{1}{4}$ and intercept -2.173 MeV, omitted from the smearing-off plot to avoid obscuring the data. Features such as deviation from the red line, width and position of the loci are much better reproduced when smearing effects are properly included. The width of the loci generated using an incorrect m_A assumption that can be observed in the smearing-off plot is due to events from different levels in ^{18}O having slightly different positions on the Catania plot. The species that give rise to these loci can be identified using the Monte-Carlo simulations and are labelled on the plots.

described previously) and in the case where all smearing effects are present. It can be seen that the data are well reproduced with these considerations, but not in the case where these effects are ignored. This is necessary not just for identifying loci based on detected species, but also for identifying locations of genuine events. This is particularly important for the region highlighted in orange, where bad silicon events due to detector pile-up and charge-sharing lie very close to a locus of good events. It is vital that these good events are separated and identified in order to extract the absolute branching ratios.

4. Acknowledgements

References

[1] Hiura J, Abe Y, Saitō S and Endō O 1969 *Progr. Theor. Phys.* **42** 555-80
[2] Buck B, Johnston J C, Merchant A C and Perez S M 1995 *Phys. Rev.* C **52** 1840-44
[3] von Oerzten W *et al* 2001 *Eur. Phys. J.* A **11** 403-11
[4] von Oertzen W *et al* 2009 *Eur. Phys. J.* A **43** 17-33
[5] Morgan G 1970 *Nucl. Phys.* A **148** 480
[6] Artemov K 1983 *Sov. J. Nucl. Phys.* **37** 805
[7] Fortune H 1978 *Phys. Rev.* C **18** 1053
[8] Curtis N, Caussyn D D, Chandler C, Cooper M W, Fletcher N R, Laird R W and Pavan J 2002 *Phys. Rev.* C **66** 024315
[9] Thompson I J and Nunes F M 2009 *Nuclear Reactions for Astrophysics* (Cambridge University Press) p 303
[10] Pirrie S 2018 *Proc. 4th Int. Workshop on State of the Art in Nuclear Cluster Physics (Galveston)* vol 2038:1 (AIP Publishing) 020037
[11] Wirth H -F 2001 PhD thesis, Technischen Universität München
[12] Curtis N *et al* 1996 *Phys. Rev.* C **53** 1804-10
[13] Curtis N *et al* 1995 *Phys. Rev.* C **51** 1554-7
[14] Curtis N 1995 PhD thesis, University of Birmingham
[15] Smith R 2017 PhD thesis, University of Birmingham
[16] Wheldon C, Ashwood N I, Barr M, Curtis N, Freer M, Kokalova Tz, Malcolm J D, Spencer S J and Ziman V A 2011 *Phys. Rev.* C **83** 064324